

# Hybrid high-order methods for the wave equation

Alexandre Ern

ENPC and INRIA, Paris, France

joint work with E. Burman (UCL), G. Delay (Sorbonne), O. Duran (Bergen)

collaboration and support: CEA

ICOSAHOM, Vienna, 13/07/2021

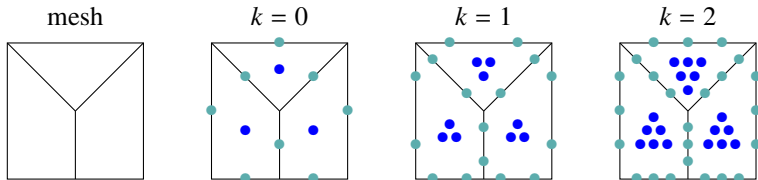
## Hybrid high-order (HHO) methods ...

- in a nutshell
- for wave propagation
- on unfitted meshes (curved interfaces/boundary)

## **HHO in a nutshell**

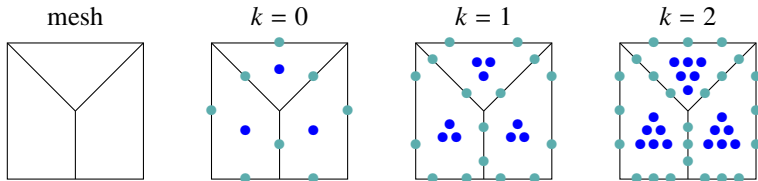
# Basic ideas

- Introduced in [Di Pietro, AE, Lemaire 14; Di Pietro, AE 15]
- Degrees of freedom (dofs) located on mesh **cells** and **faces**
- Let us start with polynomials of the **same degree  $k \geq 0$**  on **cells** and **faces**



# Basic ideas

- Introduced in [Di Pietro, AE, Lemaire 14; Di Pietro, AE 15]
- Degrees of freedom (dofs) located on mesh **cells** and **faces**
- Let us start with polynomials of the **same degree  $k \geq 0$**  on **cells** and **faces**



- In each cell, one devises a local **gradient reconstruction** operator
- One adds a **local stabilization** to weakly enforce the matching of cell dofs trace with face dofs
- The global problem is assembled cellwise as in FEM

# Gradient reconstruction and stabilization

- Mesh cell  $T \in \mathcal{T}$ , cell dofs  $u_T \in \mathbb{P}^k(T)$ , face dofs  $u_{\partial T} \in \mathbb{P}^k(\mathcal{F}_{\partial T})$

$$\hat{u}_T = (u_T, u_{\partial T}) \in \hat{U}_T := \mathbb{P}^k(T) \times \mathbb{P}^k(\mathcal{F}_{\partial T})$$

- Local potential reconstruction  $R_T : \hat{U}_T \rightarrow \mathbb{P}^{k+1}(T)$  s.t.

$$(\nabla R_T(\hat{u}_T), \nabla q)_T = -(u_T, \Delta q)_T + (u_{\partial T}, \nabla q \cdot \mathbf{n}_T)_{\partial T}, \quad \forall q \in \mathbb{P}^{k+1}(T)/\mathbb{R}$$

together with  $(R_T(\hat{u}_T), 1)_T = (u_T, 1)_T$

# Gradient reconstruction and stabilization

- Mesh cell  $T \in \mathcal{T}$ , cell dofs  $u_T \in \mathbb{P}^k(T)$ , face dofs  $u_{\partial T} \in \mathbb{P}^k(\mathcal{F}_{\partial T})$

$$\hat{u}_T = (u_T, u_{\partial T}) \in \hat{U}_T := \mathbb{P}^k(T) \times \mathbb{P}^k(\mathcal{F}_{\partial T})$$

- Local potential reconstruction  $R_T : \hat{U}_T \rightarrow \mathbb{P}^{k+1}(T)$  s.t.

$$(\nabla R_T(\hat{u}_T), \nabla q)_T = -(u_T, \Delta q)_T + (u_{\partial T}, \nabla q \cdot \mathbf{n}_T)_{\partial T}, \quad \forall q \in \mathbb{P}^{k+1}(T)/\mathbb{R}$$

together with  $(R_T(\hat{u}_T), 1)_T = (u_T, 1)_T$

- Local **gradient reconstruction**  $\mathbf{G}_T(\hat{u}_T) := \nabla R_T(\hat{u}_T) \in \nabla \mathbb{P}^{k+1}(T)$
- Local **stabilization** operator acting on  $\delta := u_T|_{\partial T} - u_{\partial T}$

$$S_{\partial T}(\hat{u}_T) := \Pi_{\partial T}^k \left( \delta - \underbrace{((I - \Pi_T^k)R_T(0, \delta))|_{\partial T}}_{\text{high-order correction}} \right)$$

- Local bilinear form for Poisson model problem

$$a_T(\hat{u}_T, \hat{w}_T) := (\mathbf{G}_T(\hat{u}_T), \mathbf{G}_T(\hat{w}_T))_T + h_T^{-1}(S_{\partial T}(\hat{u}_T), S_{\partial T}(\hat{w}_T))_{\partial T}$$

- Stability and boundedness

$$\alpha \|\hat{u}_T\|_{\hat{U}_T}^2 \leq a_T(\hat{u}_T, \hat{u}_T) \leq \omega \|\hat{u}_T\|_{\hat{U}_T}^2, \quad \forall \hat{u}_T \in \hat{U}_T$$

$$\text{with } \|\hat{u}_T\|_{\hat{U}_T}^2 := \|\nabla u_T\|_T^2 + h_T^{-1} \|u_T|_{\partial T} - u_{\partial T}\|_{\partial T}^2$$



- Local bilinear form for Poisson model problem

$$a_T(\hat{u}_T, \hat{w}_T) := (\mathbf{G}_T(\hat{u}_T), \mathbf{G}_T(\hat{w}_T))_T + h_T^{-1} (S_{\partial T}(\hat{u}_T), S_{\partial T}(\hat{w}_T))_{\partial T}$$

- Stability and boundedness

$$\alpha \|\hat{u}_T\|_{\hat{U}_T}^2 \leq a_T(\hat{u}_T, \hat{u}_T) \leq \omega \|\hat{u}_T\|_{\hat{U}_T}^2, \quad \forall \hat{u}_T \in \hat{U}_T$$

$$\text{with } \|\hat{u}_T\|_{\hat{U}_T}^2 := \|\nabla u_T\|_T^2 + h_T^{-1} \|u_T|_{\partial T} - u_{\partial T}\|_{\partial T}^2$$

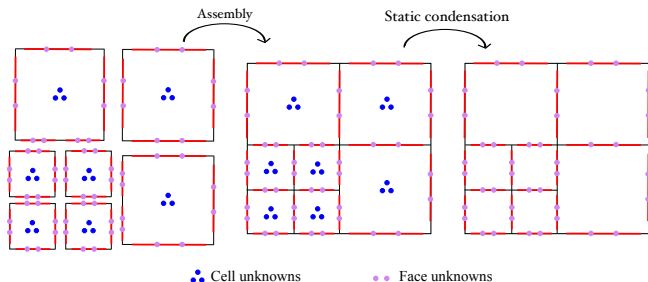
- Reduction operator  $\hat{I}_T(v) := (\Pi_T^k(v), \Pi_{\partial T}^k(v|_{\partial T})) \in \hat{U}_T, \forall v \in H^1(T)$

- Main consistency properties

- $h_T^{-1} \|v - R_T(\hat{I}_T(v))\|_T + \|\nabla(v - R_T(\hat{I}_T(v)))\|_T \lesssim h_T^{k+1} |v|_{H^{k+2}(T)}$

- $h_T^{-\frac{1}{2}} \|S_{\partial T}(\hat{I}_T(v))\|_{\partial T} \lesssim h_T^{k+1} |v|_{H^{k+2}(T)}$

# Assembly and static condensation



- Global dofs  $\hat{u}_h = (u_{\mathcal{T}}, u_{\mathcal{F}})$  ( $\mathcal{T} := \{\text{mesh cells}\}$ ,  $\mathcal{F} := \{\text{mesh faces}\}$ )

$$\hat{U}_h := \mathbb{P}^k(\mathcal{T}) \times \mathbb{P}^k(\mathcal{F}), \quad \mathbb{P}^k(\mathcal{T}) := \bigtimes_{T \in \mathcal{T}} \mathbb{P}^k(T), \quad \mathbb{P}^k(\mathcal{F}) := \bigtimes_{F \in \mathcal{F}} \mathbb{P}^k(F)$$

- Global assembly:  $\sum_{T \in \mathcal{T}} a_T(\hat{u}_T, \hat{w}_T) = \sum_{T \in \mathcal{T}} (f, w_T)_T$
- Dirichlet conditions can be directly enforced on the face boundary dofs
- Cell dofs are eliminated locally by **static condensation**
  - global problem couples only face dofs
  - cell dofs recovered by local post-processing

- **General meshes:** polytopal cells, hanging nodes
- **Optimal error estimates** (smooth solutions)
  - $O(h^{k+1})$   $H^1$ -error estimate (face dofs of order  $k \geq 0$ )
  - $O(h^{k+2})$   $L^2$ -error estimate (with full elliptic regularity)

- **General meshes:** polytopal cells, hanging nodes
- **Optimal error estimates** (smooth solutions)
  - $O(h^{k+1})$   $H^1$ -error estimate (face dofs of order  $k \geq 0$ )
  - $O(h^{k+2})$   $L^2$ -error estimate (with full elliptic regularity)
  - more generally,  $O(h^t)$   $H^1$ -error estimate if  $u \in H^{1+t}(\Omega)$ ,  $t \in (\frac{1}{2}, k+1]$
  - for  $t \in (0, \frac{1}{2})$ , see [AE, Guermond 21 (FoCM)]

- **General meshes:** polytopal cells, hanging nodes
- **Optimal error estimates** (smooth solutions)
  - $O(h^{k+1})$   $H^1$ -error estimate (face dofs of order  $k \geq 0$ )
  - $O(h^{k+2})$   $L^2$ -error estimate (with full elliptic regularity)
  - more generally,  $O(h^t)$   $H^1$ -error estimate if  $u \in H^{1+t}(\Omega)$ ,  $t \in (\frac{1}{2}, k+1]$
  - for  $t \in (0, \frac{1}{2})$ , see [AE, Guermond 21 (FoCM)]
- **Local conservation**
  - optimally convergent and algebraically balanced fluxes on faces
  - as any face-based method, balance at cell level
- **Attractive computational costs**
  - only face dofs are globally coupled
  - compact stencil

- Variant on gradient reconstruction  $\mathbf{G}_T : \hat{U}_T \rightarrow \mathbb{P}^k(T; \mathbb{R}^d)$  s.t.

$$(\mathbf{G}_T(\hat{u}_T), \mathbf{q})_T = -(u_T, \operatorname{div} \mathbf{q})_T + (u_{\partial T}, \mathbf{q} \cdot \mathbf{n}_T)_{\partial T}, \quad \forall \mathbf{q} \in \mathbb{P}^k(T; \mathbb{R}^d)$$

- **same** scalar mass matrix for **each** component of  $\mathbf{G}_T(\hat{u}_T)$
- useful for **nonlinear** problems

[Di Pietro, Droniou 17; Botti, Di Pietro, Sochala 17; Abbas, AE, Pignet 18]

- Variant on gradient reconstruction  $\mathbf{G}_T : \hat{\mathbf{U}}_T \rightarrow \mathbb{P}^k(T; \mathbb{R}^d)$  s.t.

$$(\mathbf{G}_T(\hat{\mathbf{u}}_T), \mathbf{q})_T = -(\mathbf{u}_T, \operatorname{div} \mathbf{q})_T + (\mathbf{u}_{\partial T}, \mathbf{q} \cdot \mathbf{n}_T)_{\partial T}, \quad \forall \mathbf{q} \in \mathbb{P}^k(T; \mathbb{R}^d)$$

- same scalar mass matrix for each component of  $\mathbf{G}_T(\hat{\mathbf{u}}_T)$
- useful for nonlinear problems  
[Di Pietro, Droniou 17; Botti, Di Pietro, Sochala 17; Abbas, AE, Pignet 18]
- Variants on cell dofs and stabilization
  - mixed-order setting:  $k \geq 0$  for face dofs and  $(k + 1)$  for cell dofs
  - this variant allows for the simpler Lehrenfeld–Schöberl HDG stabilization

$$S_{\partial T}(\hat{\mathbf{u}}_T) := \Pi_{\partial T}^k(\delta)$$

- another variant is  $k \geq 1$  for face dofs and  $(k - 1)$  for cell dofs

- $\text{HHO}(k = 0)$  equivalent (up to stab.) to Hybrid FV and Hybrid Mimetic Mixed methods [Eymard, Gallouet, Herbin 10; Droniou et al. 10]



- HHO( $k = 0$ ) equivalent (up to stab.) to Hybrid FV and Hybrid Mimetic Mixed methods [Eymard, Gallouet, Herbin 10; Droniou et al. 10]
- HHO fits into HDG setting [Cockburn, Di Pietro, AE 16]
  - equal-order HHO uses reconstruction in the stabilization
  - HHO allows for a simpler analysis based on  $L^2$ -projections: avoids invoking the special HDG projection

- HHO( $k = 0$ ) equivalent (up to stab.) to Hybrid FV and Hybrid Mimetic Mixed methods [Eymard, Gallouet, Herbin 10; Droniou et al. 10]
- HHO fits into HDG setting [Cockburn, Di Pietro, AE 16]
  - equal-order HHO uses reconstruction in the stabilization
  - HHO allows for a simpler analysis based on  $L^2$ -projections: avoids invoking the special HDG projection
- Similar devising of HHO and weak Galerkin methods [Wang, Ye 13]
  - weak gradient  $\leftrightarrow$  HHO grad. rec.
  - WG often uses plain LS stabilization (can be suboptimal)

- HHO( $k = 0$ ) equivalent (up to stab.) to **Hybrid FV and Hybrid Mimetic Mixed methods** [Eymard, Gallouet, Herbin 10; Droniou et al. 10]
- HHO fits into **HDG setting** [Cockburn, Di Pietro, AE 16]
  - equal-order HHO uses **reconstruction in the stabilization**
  - HHO allows for a **simpler** analysis based on  $L^2$ -projections: avoids invoking the special HDG projection
- Similar devising of HHO and **weak Galerkin** methods [Wang, Ye 13]
  - weak gradient  $\leftrightarrow$  HHO grad. rec.
  - WG often uses plain LS stabilization (can be suboptimal)
- HHO equivalent (up to stab.) to **ncVEM** [Ayuso, Manzini, Lipnikov 16]
  - HHO dof space  $\hat{U}_T$  isomorphic to virtual space  $\mathcal{V}_T$ 
$$\mathbb{P}^{k+1}(T) \subsetneq \mathcal{V}_T := \{v \in H^1(T) \mid \Delta v \in \mathbb{P}^k(T), \mathbf{n} \cdot \nabla v|_{\partial T} \in \mathbb{P}^k(\mathcal{F}_{\partial T})\}$$
  - HHO grad. rec.  $\leftrightarrow$  computable gradient projection
  - stabilization controls energy-norm of noncomputable remainder
  - see [Cockburn, Di Pietro, AE 16; Di Pietro, Droniou, Manzini 18; Lemaire 21]]

- HHO( $k = 0$ ) equivalent (up to stab.) to **Hybrid FV and Hybrid Mimetic Mixed methods** [Eymard, Gallouet, Herbin 10; Droniou et al. 10]
- HHO fits into **HDG setting** [Cockburn, Di Pietro, AE 16]
  - equal-order HHO uses **reconstruction in the stabilization**
  - HHO allows for a **simpler** analysis based on  $L^2$ -projections: avoids invoking the special HDG projection
- Similar devising of HHO and **weak Galerkin** methods [Wang, Ye 13]
  - weak gradient  $\leftrightarrow$  HHO grad. rec.
  - WG often uses plain LS stabilization (can be suboptimal)
- HHO equivalent (up to stab.) to **ncVEM** [Ayuso, Manzini, Lipnikov 16]
  - HHO dof space  $\hat{\mathcal{U}}_T$  isomorphic to virtual space  $\mathcal{V}_T$ 
$$\mathbb{P}^{k+1}(T) \subsetneq \mathcal{V}_T := \{v \in H^1(T) \mid \Delta v \in \mathbb{P}^k(T), \mathbf{n} \cdot \nabla v|_{\partial T} \in \mathbb{P}^k(\mathcal{F}_{\partial T})\}$$
  - HHO grad. rec.  $\leftrightarrow$  computable gradient projection
  - stabilization controls energy-norm of noncomputable remainder
  - see [Cockburn, Di Pietro, AE 16; Di Pietro, Droniou, Manzini 18; Lemaire 21]]

- **Different devising viewpoints should be mutually enriching**

# Applications, libraries, textbooks

- **Broad area of applications** (non-exhaustive list...)
  - **solid mechanics**: nonlinear elasticity, hyperelasticity and plasticity, contact, Tresca friction, obstacle pb
  - **fluid mechanics/porous media**: Stokes, NS, poroelasticity, fractures
  - Leray-Lions, spectral pb,  $H^{-1}$ -loads, magnetostatics, de Rham complexes
- **Libraries**
  - industry (**code\_aster**, **code\_saturne**, EDF R&D), ongoing developments at CEA
  - academia: **diskpp (C++)** (ENPC/INRIA [github.com/wareHHouse](https://github.com/wareHHouse)), **HArD::Core** (Monash/Montpellier [github.com/jdroniou/HArDCore](https://github.com/jdroniou/HArDCore))
- **Textbooks**
  - **Di Pietro, Droniou**, **The HHO method for polytopal meshes. Design, analysis and applications** (Springer, 2020)
  - **Cicuttin, AE, Pignet**, **HHO methods. A primer with application to solid mechanics** (Springer Briefs, 2021)

## HHO for wave propagation

- Second-order formulation in time: Newmark schemes
- First-order formulation in time: RK schemes
- [Burman, Duran, AE 21 (CAMC)], [Burman, Duran, AE, Steins 21 (JSC)]

## Second-order formulation in time

- Domain  $\Omega \subset \mathbb{R}^d$ , time interval  $J := (0, T_f)$ ,  $T_f > 0$
- **Acoustic wave equation** with wave speed  $c := \sqrt{\kappa/\rho}$

$$\frac{1}{\kappa} \partial_{tt} p - \operatorname{div} \left( \frac{1}{\rho} \nabla p \right) = f \quad \text{in } J \times \Omega$$

Everything can be extended to **elastodynamics**

- **Weak form:** Under mild regularity assumptions on the data,

$$(\partial_{tt} p(t), w)_{\frac{1}{\kappa}; \Omega} + (\nabla p(t), \nabla w)_{\frac{1}{\rho}; \Omega} = (f(t), w)_{\Omega}, \quad \forall w \in H_0^1(\Omega) \forall t \in J$$

- **Energy balance:**  $\mathfrak{E}(t) = \mathfrak{E}(0) + \int_0^t (f(s), \partial_t p(s))_{\Omega} ds$  with

$$\mathfrak{E}(t) := \frac{1}{2} \|\partial_t p(t)\|_{\frac{1}{\kappa}; \Omega}^2 + \frac{1}{2} \|\nabla p(t)\|_{\frac{1}{\rho}; \Omega}^2$$

- Local cell dofs in  $\mathbb{P}^{k'}(T)$ ,  $k' \in \{k, k+1\}$ , and local face dofs in  $\mathbb{P}^k(\mathcal{F}_{\partial T})$

$$\hat{u}_T = (u_T, u_{\partial T}) \in \hat{U}_T := \mathbb{P}^{k'}(T) \times \mathbb{P}^k(\mathcal{F}_{\partial T})$$

- Local gradient reconstruction  $\mathbf{G}_T(\hat{u}_T) \in \mathbb{P}^k(T; \mathbb{R}^d)$  (or in  $\nabla \mathbb{P}^{k+1}(T)$ )
- Local stabilization acting on  $\delta := u_T|_{\partial T} - u_{\partial T}$

$$S_{\partial T}(\hat{u}_T) := \begin{cases} \Pi_{\partial T}^k(\delta - ((I - \Pi_T^k)R_T(0, \delta))|_{\partial T}) & \text{if } k' = k \\ \Pi_{\partial T}^k(\delta) & \text{if } k' = k+1 \end{cases}$$

- Local bilinear form

$$a_T(\hat{u}_T, \hat{w}_T) := (\mathbf{G}_T(\hat{u}_T), \mathbf{G}_T(\hat{w}_T))_{\frac{1}{\rho}; T} + \tau_{\partial T}(S_{\partial T}(\hat{u}_T), S_{\partial T}(\hat{w}_T))_{\partial T}$$

with  $\tau_{\partial T} := (\rho|_T h_T)^{-1}$



- Global dofs  $\hat{\mathbf{u}}_h = (\mathbf{u}_{\mathcal{T}}, \mathbf{u}_{\mathcal{F}}) \in \hat{\mathbf{U}}_h := \mathbb{P}^{k'}(\mathcal{T}) \times \mathbb{P}^k(\mathcal{F})$
- Global assembly leading to

$$a_h(\hat{\mathbf{u}}_h, \hat{\mathbf{w}}_h) := \sum_{T \in \mathcal{T}} a_T(\hat{\mathbf{u}}_T, \hat{\mathbf{w}}_T) := (\mathbf{G}_{\mathcal{T}}(\hat{\mathbf{u}}_h), \mathbf{G}_{\mathcal{T}}(\hat{\mathbf{w}}_h))_{\frac{1}{\rho}; \Omega} + s_h(\hat{\mathbf{u}}_h, \hat{\mathbf{w}}_h)$$

- Dirichlet conditions can be directly enforced on the face boundary dofs

$$\hat{\mathbf{U}}_{h0} := \mathbb{P}^{k'}(\mathcal{T}) \times \mathbb{P}^k(\mathcal{F}^\circ)$$

with  $\mathcal{F}^\circ := \{\text{mesh interfaces}\}$

- Wave equation in space semi-discrete form:  $\hat{p}_h \in C^2(\bar{J}; \hat{U}_{h0})$  s.t.

$$(\partial_{tt} p_{\mathcal{T}}(t), w_{\mathcal{T}})_{\frac{1}{\kappa}; \Omega} + a_h(\hat{p}_h(t), \hat{w}_h) = (f(t), w_{\mathcal{T}})_{\Omega}, \quad \forall \hat{w}_h \in \hat{U}_{h0} \quad \forall t \in J$$

- Wave equation in space semi-discrete form:  $\hat{p}_h \in C^2(\bar{J}; \hat{U}_{h0})$  s.t.

$$(\partial_{tt} p_{\mathcal{T}}(t), w_{\mathcal{T}})_{\frac{1}{\kappa}; \Omega} + a_h(\hat{p}_h(t), \hat{w}_h) = (f(t), w_{\mathcal{T}})_{\Omega}, \quad \forall \hat{w}_h \in \hat{U}_{h0} \quad \forall t \in J$$

- Energy balance:  $\mathfrak{E}_h(t) = \mathfrak{E}_h(0) + \int_0^t (f(s), \partial_t p_{\mathcal{T}}(s))_{\Omega} ds$  with

$$\mathfrak{E}_h(t) := \frac{1}{2} \|\partial_t p_{\mathcal{T}}(t)\|_{\frac{1}{\kappa}; \Omega}^2 + \frac{1}{2} \|\mathbf{G}_{\mathcal{T}}(\hat{p}_h(t))\|_{\frac{1}{\rho}; \Omega}^2 + \frac{1}{2} s_h(\hat{p}_h(t), \hat{p}_h(t))$$

Stabilization is taken into account in the energy definition

- HDG methods for wave equation in second-order form [Cockburn, Fu, Hungria, Ji, Sanchez, Sayas 18]

- Bases for  $\mathbb{P}^k(\mathcal{T})$  and  $\mathbb{P}^k(\mathcal{F})$ , component vector  $(\mathbf{P}_{\mathcal{T}}(t), \mathbf{P}_{\mathcal{F}}(t)) \in \mathbb{R}^{N_{\mathcal{T}} \times N_{\mathcal{F}}}$

$$\begin{bmatrix} \mathbf{M}_{\mathcal{T}\mathcal{T}} \partial_{tt} \mathbf{P}_{\mathcal{T}}(t) \\ 0 \end{bmatrix} + \begin{bmatrix} \mathbf{K}_{\mathcal{T}\mathcal{T}} & \mathbf{K}_{\mathcal{T}\mathcal{F}} \\ \mathbf{K}_{\mathcal{F}\mathcal{T}} & \mathbf{K}_{\mathcal{F}\mathcal{F}} \end{bmatrix} \begin{bmatrix} \mathbf{P}_{\mathcal{T}}(t) \\ \mathbf{P}_{\mathcal{F}}(t) \end{bmatrix} = \begin{bmatrix} \mathbf{F}_{\mathcal{T}}(t) \\ 0 \end{bmatrix}$$

- Mass matrix  $\mathbf{M}_{\mathcal{T}\mathcal{T}}$  and stiffness submatrix  $\mathbf{K}_{\mathcal{T}\mathcal{T}}$  are **block-diagonal**
- Stiffness submatrix  $\mathbf{K}_{\mathcal{F}\mathcal{F}}$  is only sparse: **face dofs from the same cell are coupled together** owing to reconstruction

- Assuming a smooth solution,
  - $\|\partial_t p - \partial_t p_{\mathcal{T}}\|_{L^\infty(J; L^2(\frac{1}{\kappa}; \Omega))} + \|\nabla p - \mathbf{G}_{\mathcal{T}}(\hat{p}_h)\|_{L^2(J; L^2(\frac{1}{\rho}; \Omega))}$  decays as  $O(h^{k+1})$
  - $\|\Pi_{\mathcal{T}}^{k'}(p) - p_{\mathcal{T}}\|_{L^\infty(J; L^2(\frac{1}{\rho}; \Omega))}$  decays as  $O(h^{k+2})$  under (full) elliptic reg.
- Some comments on proofs
  - adapt ideas for FEM analysis from [Dupont 73; Wheeler 73; Baker 76]
  - simpler than for HDG (avoids HDG projection which needs a **special initialization** in HDG scheme)
  - could be re-used in DG setting using discrete gradients (revisiting [Grote, Schneebeli, Schötzau 06])

- Newmark scheme with parameters  $(\beta, \gamma) = (\frac{1}{4}, \frac{1}{2})$ 
  - **implicit, second-order, unconditionally stable**
  - $p, \partial_t p, \partial_{tt} p$  are approximated by **hybrid pairs**  $\hat{p}_h^n, \hat{v}_h^n, \hat{a}_h^n \in \hat{U}_{h0}, \forall n \geq 0$
- Each time-step implemented as usual

- Newmark scheme with parameters  $(\beta, \gamma) = (\frac{1}{4}, \frac{1}{2})$ 
  - **implicit, second-order, unconditionally stable**
  - $p, \partial_t p, \partial_{tt} p$  are approximated by **hybrid pairs**  $\hat{p}_h^n, \hat{v}_h^n, \hat{a}_h^n \in \hat{U}_{h0}, \forall n \geq 0$
- Each time-step implemented as usual
- Discrete energy is **exactly conserved**
- Central FD scheme is not efficient: inversion of stiffness submatrix  $K_{\mathcal{FF}}$

# First-order formulation in time

- Introduce velocity  $v := \partial_t p$  and dual variable  $\sigma := \frac{1}{\rho} \nabla p$

$$\begin{cases} \rho \partial_t \sigma - \nabla v = 0 \\ \frac{1}{\kappa} \partial_t v - \operatorname{div} \sigma = f \end{cases} \quad \text{in } J \times \Omega$$

- **Weak form:**  $\forall (\tau, w) \in L^2(\Omega; \mathbb{R}^d) \times H_0^1(\Omega), \forall t \in J,$

$$\begin{cases} (\partial_t \sigma(t), \tau)_{\rho; \Omega} - (\nabla v(t), \tau)_{\Omega} = 0 \\ (\partial_t v(t), w)_{\frac{1}{\kappa}; \Omega} + (\sigma(t), \nabla w)_{\Omega} = (f(t), w)_{\Omega} \end{cases}$$

- **Energy balance:**  $\mathfrak{E}(t) = \mathfrak{E}(0) + \int_0^t (f(s), v(s))_{\Omega} ds$  with

$$\mathfrak{E}(t) := \frac{1}{2} \|v(t)\|_{\frac{1}{\kappa}; \Omega}^2 + \frac{1}{2} \|\sigma(t)\|_{\rho; \Omega}^2$$



# HHO space semi-discretization

- $\hat{\mathbf{v}}_h \in C^1(\bar{J}; \hat{\mathbf{U}}_{h0})$  and  $\boldsymbol{\sigma}_{\mathcal{T}} \in C^1(\bar{J}; \mathbf{S}_{\mathcal{T}})$  with  $\mathbf{S}_{\mathcal{T}} := \mathbb{P}^k(\mathcal{T}; \mathbb{R}^d)$
- Space semi-discrete form:

$$\begin{cases} (\partial_t \boldsymbol{\sigma}_{\mathcal{T}}(t), \boldsymbol{\tau}_{\mathcal{T}})_{\rho; \Omega} - (\mathbf{G}_{\mathcal{T}}(\hat{\mathbf{v}}_h(t)), \boldsymbol{\tau}_{\mathcal{T}})_{\Omega} = 0 \\ (\partial_t \mathbf{v}_{\mathcal{T}}(t), \mathbf{w}_{\mathcal{T}})_{\frac{1}{\kappa}; \Omega} + (\boldsymbol{\sigma}_{\mathcal{T}}(t), \mathbf{G}_{\mathcal{T}}(\hat{\mathbf{w}}_h))_{\Omega} + \tilde{s}_h(\hat{\mathbf{v}}_h(t), \hat{\mathbf{w}}_h) = (f(t), \mathbf{w}_{\mathcal{T}})_{\Omega} \end{cases}$$

- Stabilization  $\tilde{s}_h(\cdot, \cdot)$  with weight  $\tilde{\tau}_{\partial T} = (\rho c)_{|T}^{-1}$ , i.e.,  $\tilde{\tau}_{\partial T} = O(1)$

- $\hat{\mathbf{v}}_h \in C^1(\bar{J}; \hat{\mathbf{U}}_{h0})$  and  $\boldsymbol{\sigma}_{\mathcal{T}} \in C^1(\bar{J}; \mathbf{S}_{\mathcal{T}})$  with  $\mathbf{S}_{\mathcal{T}} := \mathbb{P}^k(\mathcal{T}; \mathbb{R}^d)$
- Space semi-discrete form:

$$\begin{cases} (\partial_t \boldsymbol{\sigma}_{\mathcal{T}}(t), \boldsymbol{\tau}_{\mathcal{T}})_{\rho; \Omega} - (\mathbf{G}_{\mathcal{T}}(\hat{\mathbf{v}}_h(t)), \boldsymbol{\tau}_{\mathcal{T}})_{\Omega} = 0 \\ (\partial_t \mathbf{v}_{\mathcal{T}}(t), \mathbf{w}_{\mathcal{T}})_{\frac{1}{\kappa}; \Omega} + (\boldsymbol{\sigma}_{\mathcal{T}}(t), \mathbf{G}_{\mathcal{T}}(\hat{\mathbf{w}}_h))_{\Omega} + \tilde{s}_h(\hat{\mathbf{v}}_h(t), \hat{\mathbf{w}}_h) = (f(t), \mathbf{w}_{\mathcal{T}})_{\Omega} \end{cases}$$

- Stabilization  $\tilde{s}_h(\cdot, \cdot)$  with weight  $\tilde{\tau}_{\partial T} = (\rho c)_{|T}^{-1}$ , i.e.,  $\tilde{\tau}_{\partial T} = O(1)$
- Energy balance:  $\mathfrak{E}_h(t) + \int_0^t \tilde{s}_h(\hat{\mathbf{v}}_h(s), \hat{\mathbf{v}}_h(s)) ds = \mathfrak{E}_h(0) + \int_0^t (f(s), \mathbf{v}_{\mathcal{T}}(s))_{\Omega} ds$

$$\mathfrak{E}_h(t) := \frac{1}{2} \|\mathbf{v}_{\mathcal{T}}(t)\|_{\frac{1}{\kappa}; \Omega}^2 + \frac{1}{2} \|\boldsymbol{\sigma}_{\mathcal{T}}(t)\|_{\rho; \Omega}^2$$

Stabilization acts as a dissipative mechanism

- HDG methods for wave equation in first-order form [Nguyen, Peraire, Cockburn 11; Strangmeier, Nguyen, Peraire, Cockburn 16]

- Component vectors  $\mathbf{Z}_{\mathcal{T}}(t) \in \mathbb{R}^{M_{\mathcal{T}}}$  and  $(\mathbf{V}_{\mathcal{T}}(t), \mathbf{V}_{\mathcal{F}}(t)) \in \mathbb{R}^{N_{\mathcal{T}} \times N_{\mathcal{F}}}$

$$\begin{bmatrix} \mathbf{M}_{\mathcal{T}\mathcal{T}}^{\sigma} \partial_t \mathbf{Z}_{\mathcal{T}}(t) \\ \mathbf{M}_{\mathcal{T}\mathcal{T}} \partial_t \mathbf{V}_{\mathcal{T}}(t) \\ 0 \end{bmatrix} + \begin{bmatrix} 0 & -\mathbf{G}_{\mathcal{T}} & -\mathbf{G}_{\mathcal{F}} \\ \mathbf{G}_{\mathcal{T}}^{\dagger} & \mathbf{S}_{\mathcal{T}\mathcal{T}} & \mathbf{S}_{\mathcal{T}\mathcal{F}} \\ \mathbf{G}_{\mathcal{F}}^{\dagger} & \mathbf{S}_{\mathcal{F}\mathcal{T}} & \mathbf{S}_{\mathcal{F}\mathcal{F}} \end{bmatrix} \begin{bmatrix} \mathbf{Z}_{\mathcal{T}}(t) \\ \mathbf{V}_{\mathcal{T}}(t) \\ \mathbf{V}_{\mathcal{F}}(t) \end{bmatrix} = \begin{bmatrix} 0 \\ \mathbf{F}_{\mathcal{T}}(t) \\ 0 \end{bmatrix}$$

- Mass matrices  $\mathbf{M}_{\mathcal{T}\mathcal{T}}^{\sigma}$  and  $\mathbf{M}_{\mathcal{T}\mathcal{T}}$  are **block-diagonal**
- Key point: stab. submatrix  $\mathbf{S}_{\mathcal{F}\mathcal{F}}$  **block-diagonal only if  $k' = k + 1$** 
  - for  $k' = k$ , high-order HHO correction in stabilization destroys this property (couples all faces of the same cell!)

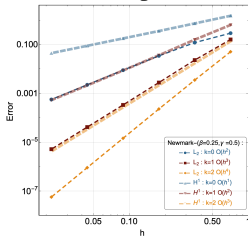
# Runge–Kutta (RK) schemes

- Natural choice for first-order formulation in time
  - **single diagonally implicit RK**: SDIRK( $s, s + 1$ ) ( $s$  stages, order  $(s + 1)$ )
  - **explicit RK**: ERK( $s$ ) ( $s$  stages, order  $s$ )
- ERK schemes subject to CFL stability condition  $\frac{c\Delta t}{h} \leq \beta(s)\mu(k)$ 
  - $\beta(s)$  slightly increases with  $s \in \{2, 3, 4\}$
  - $\mu(k)$  essentially behaves as  $(k + 1)^{-1}$  w.r.t. polynomial degree

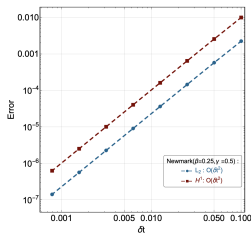
# Numerical results: homogeneous media (1/2)

- Smooth solution
- Newmark scheme (equal-order, quadrilateral mesh)

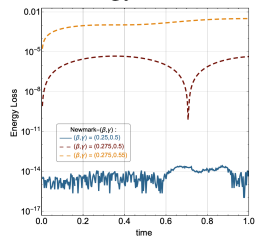
cv. in space



cv. in time



energy cons.

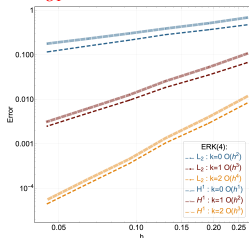


# Numerical results: homogeneous media (2/2)

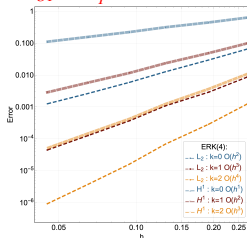
- SDIRK(3,4) and ERK(4) schemes (mixed-order, quad/poly meshes)

- recall that  $\tilde{\tau}_{\partial T} = O(1)$
- we also consider over-penalty with  $\tilde{\tau}_{\partial T} = O(h_T^{-1})$

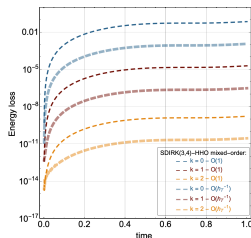
$\tilde{\tau}_{\partial T} = O(1)$ , ERK(4), poly mesh



$\tilde{\tau}_{\partial T} = O(h_T^{-1})$ , ERK(4), poly mesh



energy, SDIRK(3,4), quad mesh

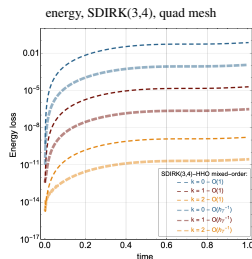
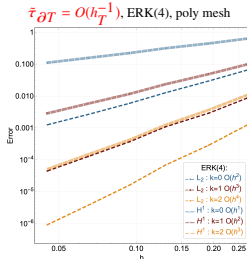
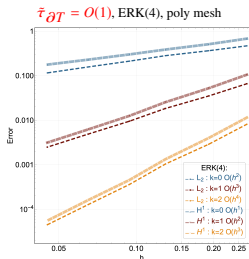


- Energy dissipation strongly tempered by increasing polynomial degree

# Numerical results: homogeneous media (2/2)

- SDIRK(3,4) and ERK(4) schemes (mixed-order, quad/poly meshes)

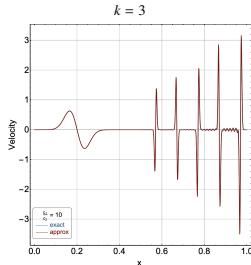
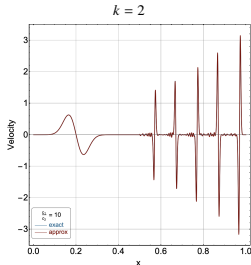
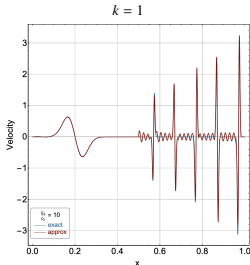
- recall that  $\tilde{\tau}_{\partial T} = O(1)$
- we also consider over-penalty with  $\tilde{\tau}_{\partial T} = O(h_T^{-1})$



- Energy dissipation strongly tempered by increasing polynomial degree
- Discussion on  $\tilde{\tau}_{\partial T}$ 
  - energy-error decays optimally as  $O(h^{k+1})$  for **both**  $\tilde{\tau}_{\partial T}$   
 $\Rightarrow$  proof for (HHO,  $O(h_T^{-1})$ ) and HDG, but using different tools
  - $L^2$ -error decays optimally as  $O(h^{k+2})$  only for  $\tilde{\tau}_{\partial T} = O(h_T^{-1})$   
 $\Rightarrow$  HDG,  $\tilde{\tau}_{\partial T} = O(1)$ , special post-proc. [Cockburn, Quenneville-Bélair 12]
  - $\tilde{\tau}_{\partial T} = O(h_T^{-1})$  worsens CFL condition for ERK schemes

# Numerical results: heterogeneous media (1/3)

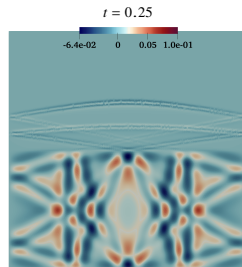
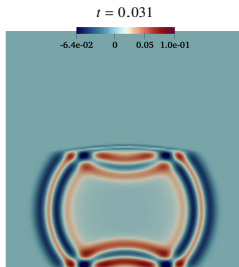
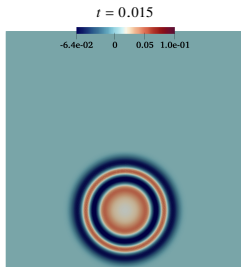
- 1D test case,  $\Omega_1 = (0, 0.5)$ ,  $\Omega_2 = (0.5, 1)$ ,  $c_1/c_2 = 10$ 
  - initial Gaussian profile in  $\Omega_1$
  - analytical solution available (series)
- Benefits of increasing polynomial degree
  - Newmark scheme, equal-order,  $k \in \{1, 2, 3\}$ ,  $h = 0.1 \times 2^{-8}$ ,  $\Delta t = 0.1 \times 2^{-9}$
  - HHO-Newmark solution at  $t = \frac{1}{2}$  (after reflection/transmission at  $x = \frac{1}{2}$ )





# Numerical results: heterogeneous media (2/3)

- 2D test case, **Ricker (Mexican hat) wavelet**
  - $\Omega_1 = (0, 1) \times (0, \frac{1}{2})$ ,  $\Omega_2 = (0, 1) \times (\frac{1}{2}, 1)$ ,  $c_1/c_2 = 5$
  - $p_0 = 0$ ,  $v_0 = -\frac{4}{10} \sqrt{\frac{10}{3}} \left(1600 r^2 - 1\right) \pi^{-\frac{1}{4}} \exp\left(-800 r^2\right)$ ,  
 $r^2 = (x - x_c)^2 + (y - y_c)^2$ ,  $(x_c, y_c) = (\frac{1}{2}, \frac{1}{4}) \in \Omega_1$
  - semi-analytical solution (infinite media): gar6more2d software (INRIA)
- HHO-SDIRK(3,4) velocity profiles
  - mixed-order,  $k = 5$ , polygonal meshes
  - $\Delta t = 0.025 \times 2^{-6}$  (four times larger than Newmark for similar accuracy)



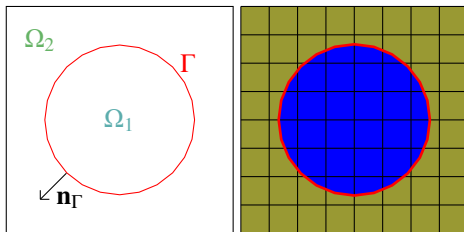
## Numerical results: heterogeneous media (3/3)

- Comparison of **computational efficiency**
  - all schemes tuned to comparable max. rel. error on a sensor at  $(\frac{1}{2}, \frac{2}{3})$
  - **very preliminary results!** (on-the-shelf solvers)
  - if no direct solvers allowed, **ERK(4) wins** despite CFL restriction
  - with direct solvers, **SDIRK(3,4) wins**
  - RK schemes **more efficient** than Newmark scheme
  - for SDIRK(3,4),  $\tilde{\tau}_{\partial T} = O(h^{-1})$  more accurate/expensive than  $\tilde{\tau}_{\partial T} = O(1)$

scheme	$(k', k)$	stab	solver	t/step	steps	time	err
ERK(4)	(6, 5)	$O(1)$	n/a	0.410	5,120	2,099	2.23
Newmark	(7, 6)	$O(h^{-1})$	iter	56.74	2,560	58,265	2.15
SDIRK(3, 4)	(6, 5)	$O(h^{-1})$	iter	31.24	640	5,639	2.21
SDIRK(3, 4)	(6, 5)	$O(1)$	iter	22.52	640	2,200	4.45
Newmark	(7, 6)	$O(h^{-1})$	direct	0.515	2,560	1,318	2.15
SDIRK(3, 4)	(6, 5)	$O(h^{-1})$	direct	1.579	640	1,010	2.21

## **Unfitted meshes**

# Elliptic interface problem



- Polytopal domain  $\Omega \subset \mathbb{R}^d$ ,  $d \in \{2, 3\}$
- Subdomains  $\Omega_1, \Omega_2 \subset \Omega$  with different (contrasted) material properties
- Curved interface  $\Gamma$ , jump  $\llbracket a \rrbracket_\Gamma = a|_{\Omega_1} - a|_{\Omega_2}$
- Model problem

$$\begin{aligned} -\operatorname{div}(\kappa \nabla u) &= f && \text{in } \Omega_1 \cup \Omega_2 \\ \llbracket u \rrbracket_\Gamma &= g_D, \quad \llbracket \kappa \nabla u \rrbracket_\Gamma \cdot \mathbf{n}_\Gamma = g_N && \text{on } \Gamma \\ u &= 0 && \text{on } \partial\Omega \end{aligned}$$

- Everything can be adapted to a **single domain with curved boundary**

# Motivation for unfitted meshes

- Use of unfitted meshes for interface problems
  - curved interface can cut arbitrarily through mesh cells
  - numerical method must deal with badly cut cells
- Classical FEM on unfitted meshes
  - double unknowns in cut cells and use a consistent Nitsche's penalty technique to enforce jump conditions [Hansbo, Hansbo 02]
  - ghost penalty [Burman 10] to counter bad cuts (gradient jump penalty across faces near curved boundary/interface)

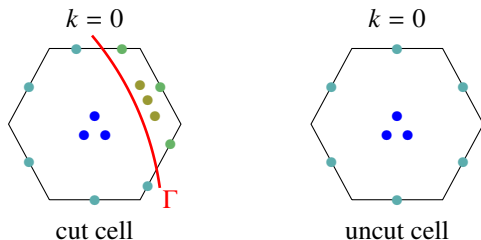
# Motivation for unfitted meshes

- Use of **unfitted meshes** for interface problems
  - curved interface can cut arbitrarily through mesh cells
  - numerical method must deal with **badly cut cells**
- Classical FEM on unfitted meshes
  - double unknowns in cut cells and use a **consistent Nitsche's penalty** technique to enforce jump conditions [Hansbo, Hansbo 02]
  - **ghost penalty** [Burman 10] to counter bad cuts (gradient jump penalty across faces near curved boundary/interface)
- An alternative to ghost penalty: **local cell agglomeration**
  - natural for polytopal methods as dG [Sollie, Bokhove, van der Vegt 11; Johansson, Larson 13]
  - cG agglomeration procedure in [Badia, Verdugo, Martín 18]

- Main ideas [Burman, AE 18 (SINUM)]
  - double cell and face dofs in cut cells, **no dofs on curved boundary/interface**
  - **local cell agglomeration** to counter bad cuts
  - **mixed-order setting**:  $k \geq 0$  for face dofs and  $(k + 1)$  for cell dofs

- Main ideas [Burman, AE 18 (SINUM)]
  - double cell and face dofs in cut cells, **no dofs on curved boundary/interface**
  - **local cell agglomeration** to counter bad cuts
  - **mixed-order setting**:  $k \geq 0$  for face dofs and  $(k + 1)$  for cell dofs
- Improvements in [Burman, Cicuttin, Delay, AE 21 (SISC)]
  - novel gradient reconstruction, avoiding that the penalty parameter in Nitsche's method is **large enough**
  - robust cell agglomeration procedure (guaranteeing locality)
- Stokes interface problems [Burman, Delay, AE 20 (IMANUM)]
- Wave propagation [Burman, Duran, AE 21] hal-03086432

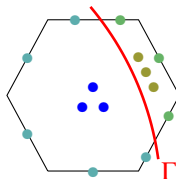




- Mesh still composed of polytopal cells (with planar faces)
- Decomposition of cut cells:  $\bar{T} = \bar{T}_1 \cup \bar{T}_2$ ,  $T^\Gamma = T \cap \Gamma$
- Decomposition of cut faces:  $\partial(T_i) = (\partial T)^i \cup T^\Gamma$ ,  $i \in \{1, 2\}$
- Local dofs (no dofs on  $T^\Gamma$ !)

$$\hat{u}_T = (u_{T_1}, u_{T_2}, u_{(\partial T)^1}, u_{(\partial T)^2}) \in \mathbb{P}^{k+1}(T_1) \times \mathbb{P}^{k+1}(T_2) \times \mathbb{P}^k(\mathcal{F}_{(\partial T)^1}) \times \mathbb{P}^k(\mathcal{F}_{(\partial T)^2})$$

# Gradient reconstruction in cut cells



- Gradient reconstruction  $\mathbf{G}_{T_i}(\hat{\mathbf{u}}_T) \in \mathbb{P}^k(T_i; \mathbb{R}^d)$  in each subcell

- (Option 1) Independent reconstruction in each subcell

$$(\mathbf{G}_{T_i}(\hat{\mathbf{u}}_T), \mathbf{q})_{T_i} = -(u_{T_i}, \operatorname{div} \mathbf{q})_{T_i} + (u_{(\partial T)^i}, \mathbf{q} \cdot \mathbf{n}_T)_{(\partial T)^i} + (u_{T_i}, \mathbf{q} \cdot \mathbf{n}_{T_i})_{T_i \Gamma}$$

- (Option 2) Reconstruction mixing data from both subcells

$$(\mathbf{G}_{T_i}(\hat{\mathbf{u}}_T), \mathbf{q})_{T_i} = -(u_{T_i}, \operatorname{div} \mathbf{q})_{T_i} + (u_{(\partial T)^i}, \mathbf{q} \cdot \mathbf{n}_T)_{(\partial T)^i} + (u_{T_{3-i}}, \mathbf{q} \cdot \mathbf{n}_{T_i})_{T_i \Gamma}$$

- Both options avoid Nitsche's consistency terms

- no penalty parameter needs to be taken large enough!

# Local bilinear form in cut cells

- Local bilinear form

$$a_T(\hat{u}_T, \hat{w}_T) := \sum_{i \in \{1,2\}} \left\{ \kappa_i (\mathbf{G}_{T_i}(\hat{u}_T), \mathbf{G}_{T_i}(\hat{w}_T))_{T_i} + s_{T_i}(\hat{u}_T, \hat{w}_T) \right\} + s_T^\Gamma(u_T, w_T)$$

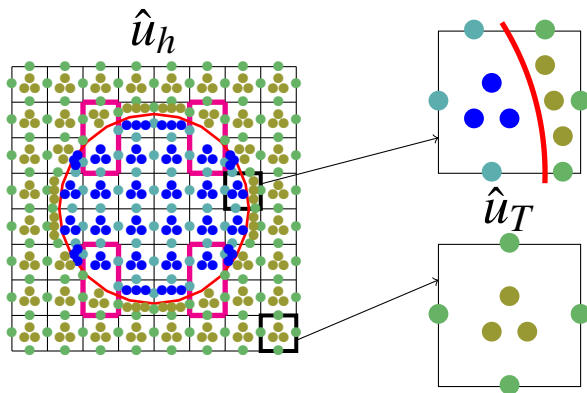
- LS stabilization inside each subdomain

$$s_{T_i}(\hat{u}_T, \hat{w}_T) := \kappa_i h_{T_i}^{-1} (\Pi_{(\partial T)^i}^k (u_{T_i}|_{(\partial T)^i} - u_{(\partial T)^i}), w_{T_i}|_{(\partial T)^i} - w_{(\partial T)^i})_{(\partial T)^i}$$

- Interface bilinear form

$$s_T^\Gamma(u_T, w_T) := \eta \kappa_1 h_T^{-1} (\llbracket u_T \rrbracket_\Gamma, \llbracket w_T \rrbracket_\Gamma)_{T^\Gamma} \text{ with } \eta = O(1)$$

- The use of two gradient reconstructions allows for **robustness w.r.t. contrast** ( $\kappa_1 \ll \kappa_2$ )
  - use option 1 in  $\Omega_1$  and option 2 in  $\Omega_2$
  - $a_T$  is symmetric, but  $\Omega_1/\Omega_2$  do not play symmetric roles



- The global dofs are in

$$\hat{u}_h \in \hat{U}_h := \bigtimes_{T \in \mathcal{T}^1} \mathbb{P}^{k+1}(T_1) \times \bigtimes_{T \in \mathcal{T}^2} \mathbb{P}^{k+1}(T_2) \times \bigtimes_{F \in \mathcal{F}^1} \mathbb{P}^k(F_1) \times \bigtimes_{F \in \mathcal{F}^2} \mathbb{P}^k(F_2)$$

- We set to zero all the face components attached to  $\partial\Omega$
- We collect in  $\hat{u}_T$  all the global unknowns related to a mesh cell  $T$

- Global problem: Find  $\hat{u}_h \in \hat{U}_h$  such that

$$a_h(\hat{u}_h, \hat{w}_h) = \ell_h(\hat{w}_h), \quad \forall \hat{w}_h \in \hat{U}_h$$

with  $a_h(\hat{u}_h, \hat{w}_h) = \sum_{T \in \mathcal{T}} a_T(\hat{u}_T, \hat{w}_T)$  and  $\ell_h(\hat{w}_h) = \sum_{T \in \mathcal{T}} \ell_T(\hat{w}_T)$  with the consistent rhs

$$\begin{aligned} \ell_T(\hat{w}_T) := & (f, w_{T_1})_{T_1} + (f, w_{T_2})_{T_2} + (g_N, w_{T_2})_{T^\Gamma} \\ & - \kappa_1 (g_D, \mathbf{G}_{T_1}(\hat{w}_T) \cdot \mathbf{n}_\Gamma + \eta h_T^{-1} \llbracket w_T \rrbracket)_{T^\Gamma} \end{aligned}$$

- All the cell dofs are eliminated locally by static condensation
- Only the face dofs are globally coupled

- Multiplicative and discrete trace inequalities [Burman, AE 18]
  - for any cut cell  $T$ , there is a ball  $T^\dagger$  of size  $O(h_T)$  containing  $T$  and a finite number of its neighbors, and s.t. all  $T \cap \Gamma$  is visible from a point in  $T^\dagger$
  - small ball with diameter  $O(h_T)$  present on both sides of interface
  - achievable using local cell agglomeration if mesh fine enough

## Error estimate

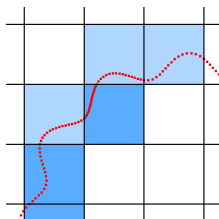
Assuming that  $u|_{\Omega_i} \in H^{1+t}(\Omega_i)$  with  $t \in (\frac{1}{2}, k+1]$ ,

$$\sum_T \sum_{i \in \{1,2\}} \kappa_i \|\nabla(u - u_{T_i})\|_{T_i}^2 \leq Ch^{2t} \sum_{i \in \{1,2\}} \kappa_i |u|_{H^{t+1}(\Omega_i)}^2$$

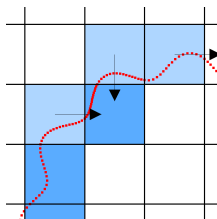
Convergence order  $O(h^{k+1})$  if  $u|_{\Omega_i} \in H^{k+2}(\Omega_i)$

# Agglomeration procedure (1/3)

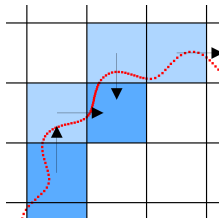
- **Three-stage** procedure with **proven locality** in the agglomeration
  - 1 for any cell KO in  $\Omega_1$ , find matching partner OK in  $\Omega_2$
  - 2 for any cell KO in  $\Omega_2$  not matched, find matching partner OK in  $\Omega_1$
  - 3 rearrange locally partnerships to avoid propagation



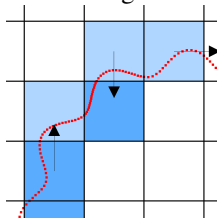
initial mesh



stage 1



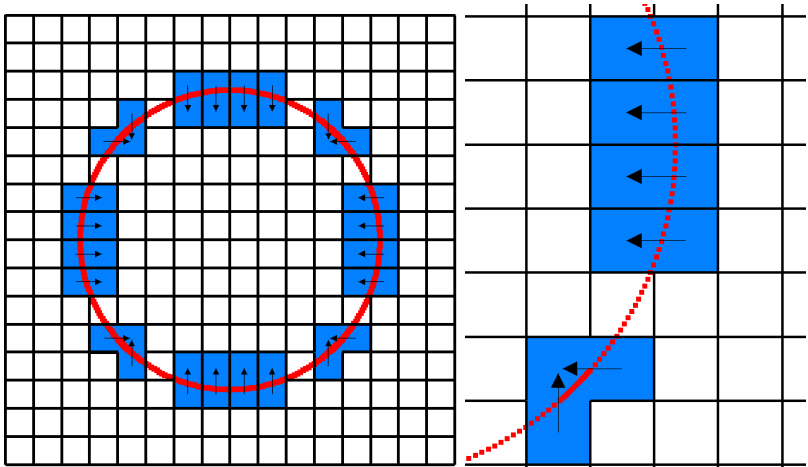
stage 2



stage 3

## Agglomeration procedure (2/3)

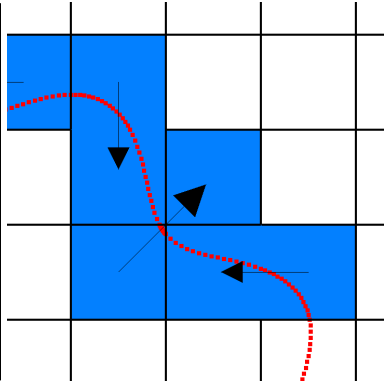
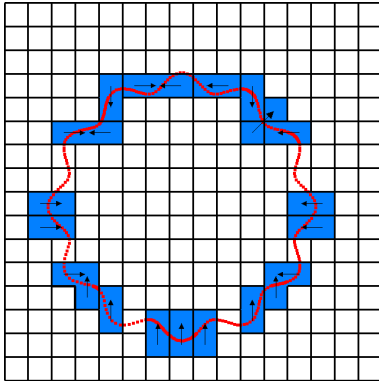
- A 16x16 mesh with circular interface





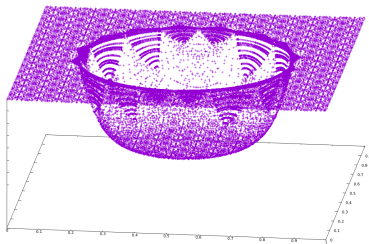
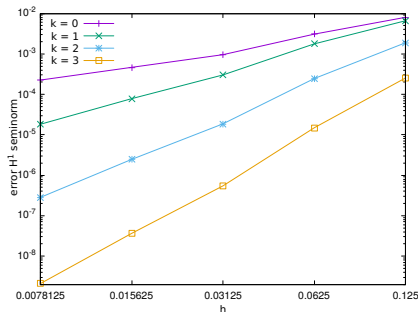
# Agglomeration procedure (3/3)

- A 16x16 mesh with flower-like interface



# Test case with contrast

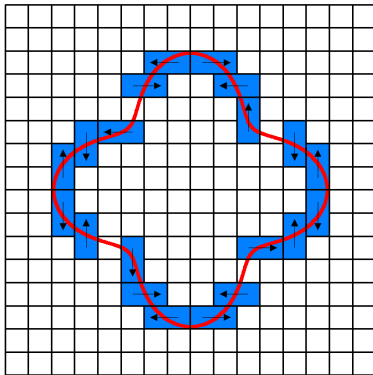
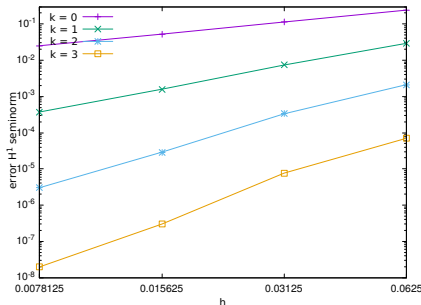
- $\kappa_1 = 1, \kappa_2 = 10^4, g_D = g_N = 0, \eta = 1$
- Circular interface ( $r^2 = (x_1 - 0.5)^2 + (x_2 - 0.5)^2$ )
- Exact solution:  $u_1 := \frac{r^6}{\kappa_1}, u_2 := \frac{r^6}{\kappa_2} + R^6(\frac{1}{\kappa_1} - \frac{1}{\kappa_2})^2$



# Test case with jump

- Flower-like interface,  $\kappa_1 = \kappa_2 = 1$
- Exact solution with jump

$$u(x_1, x_2) := \begin{cases} \sin(\pi x_1) \sin(\pi x_2) & \text{in } \Omega_1 \\ \sin(\pi x_1) \sin(\pi x_2) + 2 + x^3 y^3 & \text{in } \Omega_2 \end{cases}$$



- Subdomains  $\Omega_1, \Omega_2 \subset \Omega$ , interface  $\Gamma$ , jump  $\llbracket a \rrbracket_\Gamma = a|_{\Omega_1} - a|_{\Omega_2}$
- Acoustic wave propagation across interface

$$\begin{cases} \frac{1}{\kappa} \partial_{tt} p - \operatorname{div} \left( \frac{1}{\rho} \nabla p \right) = f & \text{in } J \times (\Omega_1 \cup \Omega_2) \\ \llbracket p \rrbracket_\Gamma = 0, \llbracket \frac{1}{\rho} \nabla p \rrbracket_\Gamma \cdot \mathbf{n}_\Gamma = 0 & \text{on } J \times \Gamma \end{cases}$$

- Main ideas as for elliptic interface problems
  - mixed-order setting  $k' = k + 1$
  - distinct gradient reconstructions  $\mathbf{G}_{T_i}$  in  $\mathbb{P}^k(T_i; \mathbb{R}^d)$ ,  $i \in \{1, 2\}$
  - LS stabilization on  $(\partial T)^i$ ,  $i \in \{1, 2\} \implies s_{T_i}(\cdot, \cdot)$

- **Second-order formulation**

$$(\partial_{tt} p_{\mathcal{T}}(t), w_{\mathcal{T}})_{\frac{1}{\kappa}; \Omega} + (\mathbf{G}_{\mathcal{T}}(\hat{p}_h(t)), \mathbf{G}_{\mathcal{T}}(\hat{w}_h))_{\frac{1}{\rho}; \Omega} + s_h^{1,2}(\hat{p}_h(t), \hat{w}_h) + s_h^{\Gamma}(p_{\mathcal{T}}(t), w_{\mathcal{T}}) = (f(t), w_{\mathcal{T}})_{\Omega}$$

- $s_h^{\Gamma}(p_{\mathcal{T}}(t), w_{\mathcal{T}}) := (\rho_1 h_T)^{-1}(\llbracket p_T \rrbracket_{\Gamma}, \llbracket w_T \rrbracket_{\Gamma})_{T^{\Gamma}}$
- Algebraic realization and **Newmark time-stepping** as in fitted case

## • Second-order formulation

$$(\partial_{tt} p_{\mathcal{T}}(t), w_{\mathcal{T}})_{\frac{1}{k}; \Omega} + (\mathbf{G}_{\mathcal{T}}(\hat{p}_h(t)), \mathbf{G}_{\mathcal{T}}(\hat{w}_h))_{\frac{1}{\rho}; \Omega} + s_h^{1,2}(\hat{p}_h(t), \hat{w}_h) + s_h^{\Gamma}(p_{\mathcal{T}}(t), w_{\mathcal{T}}) = (f(t), w_{\mathcal{T}})_{\Omega}$$

- $s_h^{\Gamma}(p_{\mathcal{T}}(t), w_{\mathcal{T}}) := (\rho_1 h_T)^{-1} (\llbracket p_T \rrbracket_{\Gamma}, \llbracket w_T \rrbracket_{\Gamma})_{T^{\Gamma}}$
- Algebraic realization and **Newmark time-stepping** as in fitted case

## • First-order formulation ( $v := \partial_t p$ , $\sigma := \frac{1}{\rho} \nabla p$ )

$$\begin{cases} (\partial_t \sigma_{\mathcal{T}}(t), \tau_{\mathcal{T}})_{\rho; \Omega} - (\mathbf{G}_{\mathcal{T}}(\hat{v}_h(t)), \tau_{\mathcal{T}})_{\Omega} = 0 \\ (\partial_t v_{\mathcal{T}}(t), w_{\mathcal{T}})_{\frac{1}{k}; \Omega} + (\sigma_{\mathcal{T}}(t), \mathbf{G}_{\mathcal{T}}(\hat{w}_h))_{\Omega} + \tilde{s}_h^{1,2}(\hat{v}_h(t), \hat{w}_h) + \tilde{s}_h^{\Gamma}(v_{\mathcal{T}}(t), w_{\mathcal{T}}) = (f(t), w_{\mathcal{T}})_{\Omega} \end{cases}$$

- $\tilde{s}_h^{\Gamma}(v_{\mathcal{T}}(t), w_{\mathcal{T}}) := \sum_{T \in \mathcal{T}_h} \tilde{\tau}_{\partial T}^{\Gamma} (\llbracket v_T \rrbracket_{\Gamma}, \llbracket w_T \rrbracket_{\Gamma})_{T^{\Gamma}}$
- $\tilde{\tau}_{\partial T}^{\Gamma} = (\rho_1 c_1)^{-1} = O(1)$  for ERK, and  $\tilde{\tau}_{\partial T}^{\Gamma} = O(h_T^{-1})$  for SDIRK
- Algebraic realization and **RK time-stepping** as in fitted case

- 2D heterogeneous test case with **flat interface**
  - $\Omega_1 := (-\frac{3}{2}, \frac{3}{2}) \times (-\frac{3}{2}, 0)$ ,  $\Omega_2 := (-\frac{3}{2}, \frac{3}{2}) \times (0, \frac{3}{2})$
  - Ricker wavelet centered at  $(0, \frac{2}{3}) \in \Omega_2$ , sensor  $S_1 = (\frac{3}{4}, -\frac{1}{3}) \in \Omega_1$
  - fitted and unfitted HHO behave similarly, both benefit from increasing  $k$

# Fitted-unfitted comparison

- 2D heterogeneous test case with **flat interface**

- $\Omega_1 := (-\frac{3}{2}, \frac{3}{2}) \times (-\frac{3}{2}, 0), \Omega_2 := (-\frac{3}{2}, \frac{3}{2}) \times (0, \frac{3}{2})$

- Ricker wavelet centered at  $(0, \frac{2}{3}) \in \Omega_2$ , sensor  $S_1 = (\frac{3}{4}, -\frac{1}{3}) \in \Omega_1$

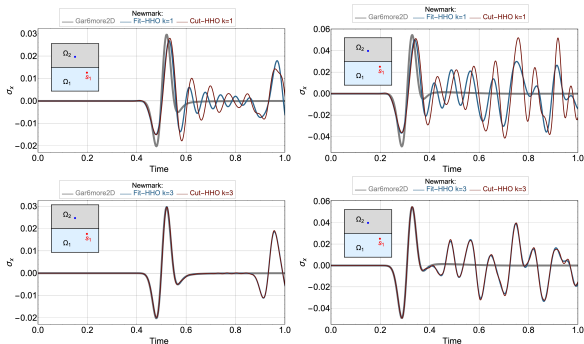
- fitted and unfitted HHO behave similarly, both benefit from increasing  $k$

- HHO-Newmark,  $\sigma_x$  signals

- comparison of semi-analytical and HHO (fitted or unfitted) solutions

- $k = 1$  (top) and  $k = 3$  (bottom)

- $c_2/c_1 = \sqrt{3}$  (low contrast, left) or  $c_2/c_1 = 8\sqrt{3}$  (high contrast, right)





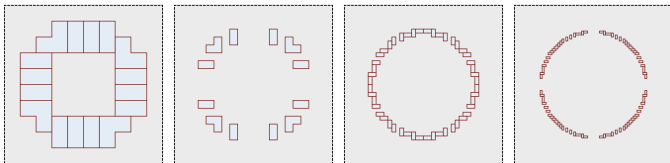
# CFL condition for ERK (1/2)

- Homogeneous test case, **flat interface**
- CFL condition for ERK(s):  $\frac{c\Delta t}{h} \leq \beta(s)\mu(k)$ 
  - $\beta(s)$  mildly depends on the number of stages
  - $\mu(k)$  behaves as  $(k+1)^{-1}$  and is quantified by solving a generalized eigenvalue problem with the mass and stiffness matrices
- Additional jump penalties in unfitted HHO **only mildly impact**  $\mu(k)$

$k$	0	1	2	3
Fitted-HHO	0.118	0.0522	0.0338	0.0229
Unfitted-HHO	0.0765	0.0373	0.0232	0.0159
Ratio	1.5	1.4	1.5	1.4

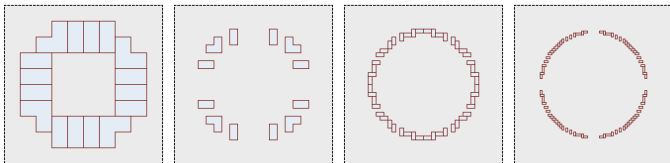
## CFL condition for ERK (2/2)

- Homogeneous test case, **circular interface**
  - study of impact of **agglomeration parameter**  $\theta_{\text{agg}}$  on  $\mu(k)$
  - “badly cut” cell flagged if relative area of any subcell falls below  $\theta_{\text{agg}}$
- Agglomerated cells for  $\theta_{\text{agg}} = 0.3$  on a sequence of refined quad meshes

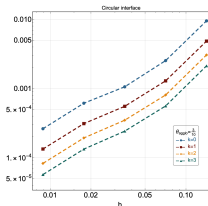


# CFL condition for ERK (2/2)

- Homogeneous test case, **circular interface**
  - study of impact of **agglomeration parameter**  $\theta_{\text{agg}}$  on  $\mu(k)$
  - “badly cut” cell flagged if relative area of any subcell falls below  $\theta_{\text{agg}}$
- Agglomerated cells for  $\theta_{\text{agg}} = 0.3$  on a sequence of refined quad meshes



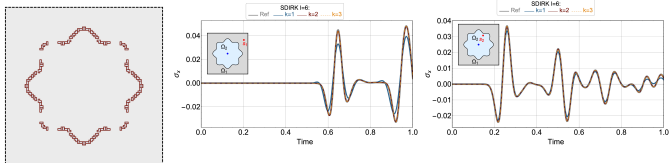
- Behavior of  $h\mu(k)$  and impact of  $\theta_{\text{agg}}$  on  $\mu(k)$ 
  - tolerating badly cut cells **deteriorates the CFL condition**



$k$	0	1	2	3
$\theta_{\text{agg}} = 0.5$	0.042	0.022	0.014	0.0099
$\theta_{\text{agg}} = 0.3$	0.030	0.015	0.0094	0.0065
Ratio	1.4	1.5	1.5	1.5
$\theta_{\text{agg}} = 0.1$	0.017	0.0087	0.0055	0.0039
Ratio	2.5	2.6	2.6	2.5

# Flower-like interface

- Agglomerated cells for a flower-like interface (quad mesh,  $h = 2^{-5}$ ), HHO-SDIRK(3,4) signal for  $\sigma_x$  at two sensors,  $k \in \{1, 2, 3\}$ ,  $c_2/c_1 = \sqrt{3}$

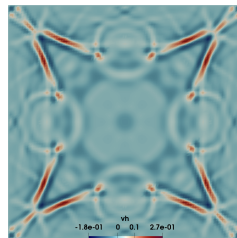
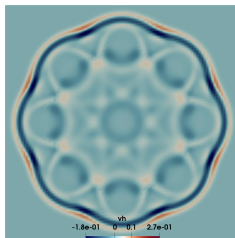
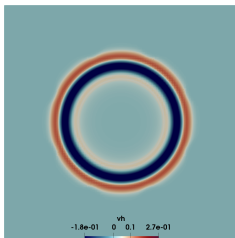


- Pressure isovalues, SDIRK(3,4),  $k = 3$ ,  $h = 0.1 \times 2^{-8}$ ,  $\Delta t = 2^{-6}$

$t = 0.25$

$t = 0.5$

$t = 1$

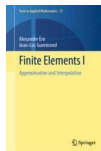


# Some references

- HHO
  - seminal papers [Di Pietro, AE, Lemaire 14; Di Pietro, AE 15]
  - textbooks [Di Pietro, Droniou, 20; Cicuttin, AE, Pignet, 21]
- HHO for wave propagation
  - [Burman, Duran, AE 21 (CAMC)], [Burman, Duran, AE, Steins 21 (JSC)]
- Unfitted HHO
  - [Burman, AE 18 (SINUM)], [Burman, Cicuttin, Delay, AE 21 (SISC)]

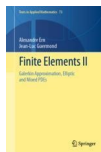
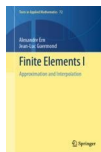
# Some references

- HHO
  - seminal papers [Di Pietro, AE, Lemaire 14; Di Pietro, AE 15]
  - textbooks [Di Pietro, Droniou, 20; Cicuttin, AE, Pignet, 21]
- HHO for wave propagation
  - [Burman, Duran, AE 21 (CAMC)], [Burman, Duran, AE, Steins 21 (JSC)]
- Unfitted HHO
  - [Burman, AE 18 (SINUM)], [Burman, Cicuttin, Delay, AE 21 (SISC)]
- **New Finite Element book(s)** (Springer, TAM vols. 72-74, 2021)  
with J.-L. Guermond, 83 chapters of 12/14 pages plus about 500 exercises



# Some references

- HHO
  - seminal papers [Di Pietro, AE, Lemaire 14; Di Pietro, AE 15]
  - textbooks [Di Pietro, Droniou, 20; Cicuttin, AE, Pignet, 21]
- HHO for wave propagation
  - [Burman, Duran, AE 21 (CAMC)], [Burman, Duran, AE, Steins 21 (JSC)]
- Unfitted HHO
  - [Burman, AE 18 (SINUM)], [Burman, Cicuttin, Delay, AE 21 (SISC)]
- **New Finite Element book(s)** (Springer, TAM vols. 72-74, 2021)  
with J.-L. Guermond, 83 chapters of 12/14 pages plus about 500 exercises



Thank you for your attention!